

OPEN

# Circulating B Cells With Memory and Antibody-Secreting Phenotypes Are Detectable in Pediatric Kidney Transplant Recipients Before the Development of Antibody-Mediated Rejection

Clara Fischman, MD,<sup>1</sup> Miguel Fribourg, PhD,<sup>1</sup> Ginevri Fabrizio, MD,<sup>2</sup> Michela Cioni, PhD,<sup>2</sup> Patrizia Comoli, MD,<sup>3</sup> Arcangelo Nocera, MD,<sup>2</sup> Massimo Cardillo, MD,<sup>4</sup> Chiara Cantarelli, MD,<sup>1,5</sup> Lorenzo Gallon, MD,<sup>6</sup> Astgik Petrosyan, PhD,<sup>7</sup> Stefano Da Sacco, PhD,<sup>7</sup> Laura Perin, PhD,<sup>7</sup> and Paolo Cravedi, MD, PhD<sup>1</sup>

**Background.** Development of anti-human leukocyte antigen donor-specific antibodies (DSAs) is associated with antibody-mediated rejection (AMR) and reduced allograft survival in kidney transplant recipients. Whether changes in circulating lymphocytes anticipate DSA or AMR development is unclear. **Methods.** We used time-of-flight mass cytometry to analyze prospectively collected peripheral blood mononuclear cells (PBMC) from pediatric kidney transplant recipients who developed DSA (DSA-positive recipients [DSA<sup>POS</sup>], n = 10). PBMC were obtained at 2 months posttransplant, 3 months before DSA development, and at DSA detection. PBMC collected at the same time points posttransplant from recipients who did not develop DSA (DSA-negative recipients [DSA<sup>NEG</sup>], n = 11) were used as controls. **Results.** DSA<sup>POS</sup> and DSA<sup>NEG</sup> recipients had similar baseline characteristics and comparable frequencies of total B and T cells. Within DSA<sup>POS</sup> recipients, there was no difference in DSA levels (mean fluorescence intensity [MFI]: 13 687 ± 4159 vs 11 375 ± 1894 in DSA<sup>POS</sup>AMR-positive recipients (AMR<sup>POS</sup>) vs DSA<sup>POS</sup>AMR-negative recipients (AMR<sup>NEG</sup>), respectively; P = 0.630), C1q binding (5 DSA<sup>POS</sup>AMR<sup>POS</sup> [100%] vs 4 DSA<sup>POS</sup>AMR<sup>NEG</sup> [80%]; P = 1.000), or C3d binding (3 DSA<sup>POS</sup>AMR<sup>POS</sup> [60%] vs 1 DSA<sup>POS</sup>AMR<sup>NEG</sup> [20%]; P = 0.520) between patients who developed AMR and those who did not. However, DSA<sup>POS</sup> patients who developed AMR (n = 5; 18.0 ± 3.6 mo post-DSA detection) had increased B cells with antibody-secreting (IgD<sup>-</sup>CD27<sup>+</sup>CD38<sup>+</sup>; P = 0.002) and memory (IgD<sup>-</sup>CD27<sup>+</sup>CD38<sup>-</sup>; P = 0.003) phenotypes compared with DSA<sup>NEG</sup> and DSA<sup>POS</sup>AMR<sup>NEG</sup> recipients at DSA detection. **Conclusions.** Despite the small sample size, our comprehensive phenotypic analyses show that circulating B cells with memory and antibody-secreting phenotypes are present at DSA onset, >1 year before biopsy-proven AMR in pediatric kidney transplant recipients.

(*Transplantation Direct* 2019;5: e481; doi: 10.1097/TXD.0000000000000914. Published online 8 August, 2019.)

Received 10 May 2019.

Accepted 16 May 2019.

<sup>1</sup> Department of Medicine, Icahn School of Medicine at Mount Sinai, New York, NY.

<sup>2</sup> Nephrology, Dialysis and Transplantation Unit, IRCCS Istituto G. Gaslini, Genova, Italy.

<sup>3</sup> Pediatric Hematology/Oncology & Cell Factory, Fondazione IRCCS Policlinico S. Matteo, Pavia, Italy.

<sup>4</sup> Department Transplantation Immunology, IRCCS Fondazione Ca' Granda, Ospedale Maggiore Policlinico, Milano, Italy.

<sup>5</sup> Dipartimento di Medicina e Chirurgia Università di Parma, UO Nefrologia, Azienda Ospedaliera-Universitaria Parma, Parma, Italy.

<sup>6</sup> Department of Medicine, Division of Nephrology, Feinberg School of Medicine, Northwestern University, Chicago, IL.

<sup>7</sup> Division of Urology GOFARR Laboratory for Organ Regenerative Research and Cell Therapeutics, Children's Hospital Los Angeles, Los Angeles, CA.

C.F. and M.F. are co-first authors.

L.P. and P. Cravedi are co-senior authors.

This work was supported by the GOFARR Foundation and the Schenkman Family. F.C. received internal funding from the Icahn School of Medicine and NIDDK-T32 DK007757-18S1; this study was also supported by a grant from Fondazione Compagnia San Paolo to M. Cioni, and a grant from IRCCS Policlinico San Matteo, Progetti Ricerca Corrente to P. Comoli.

The authors declare no conflicts of interest.

C.F. and M.F. participated in the performance of the research, data analysis, and writing of the paper. G.F., M. Cioni, P. Comoli, A.N., M. Cardillo, C.C., L.G., A.P., and S.D.S. participated in the performance of the research. L.P. participated in study design, writing of the paper, and data analysis. P. Cravedi had the original idea and participated in research design, writing of the paper, and data analysis.

Previous Presentation: This study was presented in part as oral communication at the American Society of Nephrology Renal Week; October 24th 2018 (SA-OR088); San Diego, CA and at the American Transplant Congress; 2019 (19-A-2963); Boston.

Supplemental digital content (SDC) is available for this article. Direct URL citations appear in the printed text, and links to the digital files are provided in the HTML text of this article on the journal's Web site ([www.transplantationdirect.com](http://www.transplantationdirect.com)).

Correspondence: Paolo Cravedi, MD, PhD, Icahn School of Medicine at Mount Sinai, 1 Levy Pl, 10029 New York, NY. ([paolo.cravedi@mssm.edu](mailto:paolo.cravedi@mssm.edu)).

Copyright © 2019 The Author(s). *Transplantation Direct*. Published by Wolters Kluwer Health, Inc. This is an open-access article distributed under the terms of the Creative Commons Attribution-Non Commercial-No Derivatives License 4.0 (CCBY-NC-ND), where it is permissible to download and share the work provided it is properly cited. The work cannot be changed in any way or used commercially without permission from the journal.

ISSN: 2373-8731

DOI: 10.1097/TXD.0000000000000914

Short-term kidney transplantation outcomes have improved significantly over the past decades with the implementation of induction therapies and calcineurin inhibitor (CNI)-based immunosuppression regimens.<sup>1,2</sup> While these treatments reduce episodes of acute cellular rejection, they have failed to improve long-term allograft survival, with only 50%–60% of allografts functioning after 10 years.<sup>3–6</sup> The reasons for long-term allograft failure are multifactorial, but development of de novo donor-specific anti-human leukocyte antigen (HLA) antibodies (dnDSAs) is recognized as a leading cause, affecting up to 30% of unsensitized kidney transplant recipients,<sup>7,8</sup> with 1%–10% occurring within the first year posttransplant.<sup>9–15</sup>

DSA-positive recipients (DSA<sup>POS</sup>) are at increased risk of antibody-mediated rejection (AMR), a condition that can lead to accelerated allograft failure and for which treatment strategies are still not standardized.<sup>11</sup> Highly sensitized patients with pretransplant DSA incur a substantially higher rate of AMR than their DSA-negative counterparts. However, predicting which unsensitized recipients will develop dnDSA, and of those which will suffer AMR, remains difficult.<sup>7,12,16–19</sup> Recent studies suggest that the ability of DSA to activate the complement cascade,<sup>20</sup> assessed via C1q- or C3d-binding assays, correlates with allograft loss and can help risk-stratify DSA<sup>POS</sup> recipients.<sup>21–28</sup> However, data about the utility of these measures in clinical practice have not been consistent thus far.<sup>29–32</sup>

Memory B cells are formed within germinal centers following the primary encounter with alloantigen and are able to generate an accelerated immune response upon antigen re-encounter.<sup>33–36</sup> Memory B cells are also detectable in the peripheral blood of highly sensitized recipients before and during an AMR episode, even in the absence of circulating DSA.<sup>37,38</sup> However, no study to date has comprehensively looked at the immune phenotype of immunologically naive transplant recipients to investigate whether other immunologic perturbations precede antibody development or AMR.

One reason for the lack of comprehensive immune phenotyping of transplant patients is that standard flow cytometry is limited in the number of markers that can be probed in a single experiment due to autofluorescence and spectral spillover associated with fluorophores. Time-of-flight mass cytometry (CyTOF) utilizes metal isotopes that possess unique mass spectrometry signatures enabling the analysis of up to 50 cellular markers at the same time. Furthermore, CyTOF reduces experimental variability as metal isotopes can be used to tag samples with barcodes, allowing multiple samples to be analyzed simultaneously. We used CyTOF to test the hypothesis that changes occur in the phenotype of circulating T and/or B cells before the development of DSA or AMR. To do this, we comprehensively analyzed immune phenotypes of prospectively collected peripheral blood mononuclear cells (PBMC) from pediatric kidney transplant recipients who did or did not develop dnDSA, with or without AMR.

## MATERIALS AND METHODS

### Subjects and Sample Collection

Pediatric subjects (<18 y at the time of transplant) transplanted at Gaslini Hospital in Genoa, Italy, between August 2003 and March 2013 underwent serial measurement of circulating DSA at months 1, 2, 6, 9, 12 posttransplant, and every 6 months thereafter. At the time of each DSA measurement,

patients also had PBMC collected and stored in liquid nitrogen. During the study period, 136 kidney transplants were consecutively performed.

Patients were included in this study if they were recipients of a first kidney graft and nonsensitized (Panel-reactive antibody = 0; absence of any HLA antibody (Ab) in historical sera tested before kidney transplant; n = 98). We performed a case-control study, where we analyzed serially collected PBMC aliquots at 2 months posttransplant, at the last available visit before DSA development, and at the time of first DSA detection in all the consecutive patients who developed DSA within the first 12 months after transplant (n = 10) and 11 patients who received a kidney transplant during the same time period ( $\pm 6$  mo) at the same institution but did not develop DSA during the same follow-up time posttransplant. Demographic and clinical characteristics of donors and recipients were collected up to 6 years posttransplant. The protocol has been approved by the Gaslini Hospital Institutional Review Board (IRB 867/2014).

### Patient Treatment and Management

All kidney transplant recipients received the same immunosuppressive therapy consisting of anti-CD25 antibody induction (basiliximab) and maintenance with mycophenolate mofetil and a CNI (either tacrolimus or cyclosporine) with or without steroids. Tacrolimus target trough levels were 8–10 ng/mL in the first month posttransplant, 7–9 ng/mL from months 2–3, and 6–8 ng/mL thereafter. Two-hour postdose target levels of cyclosporine in whole blood ( $C_2$ ) were 1400–1800 ng/mL in the first month posttransplant, 1200–1600 ng/mL in the second month, 1000–1400 from months 3–6, and 800–1200 thereafter (see adherence calculations in section below). Graft biopsies were performed as per clinical indication, including DSA development. Diagnosis of AMR was based on Banff 2013.<sup>39</sup>

### Detection and Characterization of HLA Abs

HLA classes I and II typing were performed as described previously.<sup>21,40</sup> Anti-HLA classes I and II IgG Abs were tested with a bead-based detection assay. We used the LABScreen Mixed kit (One Lambda; Thermo Fisher Scientific, Waltham, MA), which simultaneously detects classes I and II Abs, and the single antigen bead assays (Single Antigen kit, One Lambda; Thermo Fisher Scientific) to identify HLA classes I and II specificities.<sup>40</sup> Before testing, all sera were pretreated with disodium EDTA (final concentration 10 mM, pH 7.4; Sigma-Aldrich, Milan, Italy) to rule out underestimation of Ab mean fluorescence intensity (MFI) strength due to the prozone phenomenon.<sup>41</sup> Screening assay results above a cutoff value of 3.0 for the ratio of sample to negative control were considered positive. Single-antigen results above an MFI cutoff value of 1000 were considered positive.

Heat-inactivated patient sera were tested with C1qScreen (One Lambda; Thermo Fisher Scientific) for identification of complement-binding Abs, as described.<sup>27</sup> Ab positivity was assigned at >500 MFI. Serum samples were analyzed in a blinded fashion for the presence of C3d-binding DSAs with the single-antigen flow bead technology, according to the manufacturer's protocol (Immucor Lifecode Transplant Diagnostics, Nijlen, Belgium).<sup>26</sup>

### Adherence to CNI Therapy

Routine laboratory measurement of 2-hour postdose cyclosporine ( $C_2$ ) levels and tacrolimus trough levels in whole

blood were determined using an antibody-conjugated magnetic immunoassay method and by microparticle enzyme immunoassay based on the Abbott IMx (Abbott Laboratories, Abbott Park, IL), respectively.

Tacrolimus and cyclosporine  $C_2$  levels were collected over a period of >1 year. Inpatient variability (IPV) has been shown to be a useful surrogate for CNI adherence and a predictor of long-term kidney transplant outcomes.<sup>42-44</sup> Given the small sample size of our cohort, CNI IPV was described by the coefficient of variation (CV%) and calculated as the square root of the ratio of the variance to the mean,

$$(CV\%) = \sqrt{\left\{ \frac{\sum (X_j - \bar{X})^2}{(n-1) \bar{X}} \right\}} \times 100, \text{ which has been}$$

shown to provide an accurate estimate for these studies.<sup>42</sup> Only levels collected after 6 months posttransplant, when dosing is assumed to be stable, were included in IPV calculations.

### CyTOF Sample Preparation

Our aim was to map the peripheral blood immune system of renal transplant recipients and its evolution over time, while minimizing batch effect, to increase our ability to capture differences in frequencies of immune cell compartments. To do this, we barcoded samples collected from the same recipients at the 3 different time points with anti-CD45 antibodies conjugated to unique metal isotopes before pooling the samples together. CyTOF sample preparation was conducted as previously reported.<sup>45,46</sup> Antibodies were either purchased pre-conjugated from Fluidigm (formerly DVS Sciences) or purchased purified and conjugated in-house using MaxPar X8 Polymer Kits (Fluidigm) according to the manufacturer's instructions. Sixty-three samples (21 recipients with approximately 3 time points each) were processed in 4 separate batches using 4 barcoding antibodies for each sample (to denote patient and time point) and pooled together (Figure 1). All PBMC were stained with a panel of 35 antibodies (34 for clustering, 1 for viability; see Table S1, SDC, <http://links.lww.com/TXD/A217>).

### CyTOF Data Acquisition

CyTOF data were acquired at Icahn School of Medicine at Mount Sinai as previously reported by others.<sup>45,46</sup> Samples were suspended in deionized water containing a 1/20 dilution of EQ 4 Element Beads (Fluidigm) at a concentration of 1 million cells/mL and acquired on a CyTOF2 (Fluidigm) equipped with a SuperSampler fluidics system (Victorian Airships) at an event rate of <500 events/s. After acquisition, the data were normalized using bead-based normalization in the CyTOF software. Barcodes were demultiplexed using the Fluidigm debarcoding software. The data were gated to exclude residual normalization beads, debris, dead cells, and doublets, leaving live CD45<sup>+</sup> events for subsequent clustering and high-dimensional analyses.

### CyTOF Data Analysis

We utilized a CyTOF analysis pipeline that was previously established in our laboratory.<sup>46</sup> We first clustered cells using the Phenograph algorithm<sup>47</sup> and then curated the metaclusters obtained. The frequencies for each common population were obtained by summation of the frequencies in each metacluster and subsequently debarcoded to obtain frequencies for each time point and patient. To minimize variability in measurement, our analysis strategy was structured as follows:

1. Application of Phenograph to computationally pooled samples: we pooled in silico all labeled cells from all time points for each patient to analyze the major immune compartments (10 000 cells per time point for an average of 30 000 cells per patient); we applied Phenograph and then demultiplexed them. This allowed us to map the same subsets in all the samples, as opposed to gating each sample for each patient individually.
2. Equal contribution of the samples: to avoid bias in Phenograph for the subsets present in the samples with a greater total number of T or B cells, we sampled 500 cells per sample for the CD4<sup>+</sup> and CD8<sup>+</sup> T cell subclustering. For the B-cell compartment, not all samples had 500 cells. For the 5 recipients who had at least 1 PBMC sample with

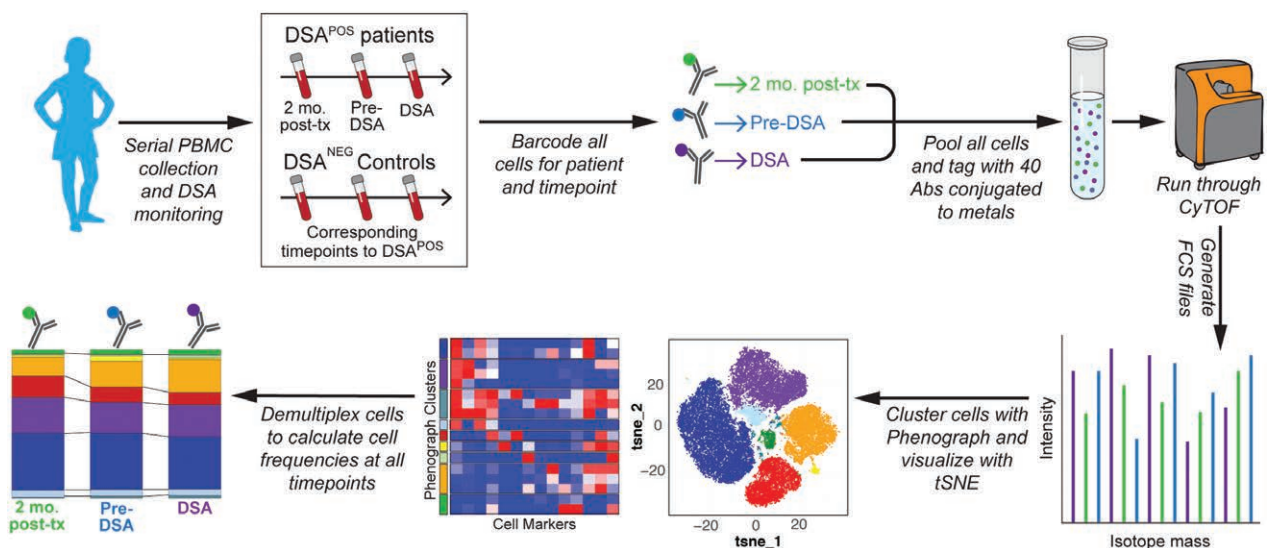


**FIGURE 1.** Study design. Blood was collected from pediatric transplant recipients every 2–3 mo to monitor DSA formation. Peripheral blood mononuclear cells (PBMC) were isolated from samples taken at 2 mo posttransplant, at the time DSA detection, and the sample just before DSA detection (corresponding time points were used for DSA<sup>NEG</sup> recipients). Cells were barcoded for patient and time, pooled, and stained with 35 antibodies conjugated to unique metal isotopes. Single-cell data acquired from time-of-flight mass cytometry (CyTOF) were clustered using Phenograph to identify cell clusters and how they evolved over time in each patient (see Materials and Methods). DSA, donor-specific antibody; DSA<sup>NEG</sup>, DSA-negative recipients; DSA<sup>POS</sup>, DSA-positive recipients; FCS, flow cytometry standard; post-tx, post-transplant; tSNE, t-distributed stochastic neighbor embedding. J Gregory @2018 printed with the permission of Mount Sinai Health System.

<500 B cells, we adjusted the contribution of cells to maximize the number of B cells analyzed. In this way, we were able to minimize clustering bias while maintaining equal contribution from each sample.

3. Reiteration: to increase power of the analyses for the cell subsets with low number of events, we reiterated the entirety of the B-cell sampling process and Phenograph clustering up to 5 times to achieve robustness in the results. Through our strategy, we effectively analyzed up to 2500 cells per sample. Despite the level of stringency imposed by the repeated sampling and clustering process, we observed little dispersion in the results indicating that our findings were robust (CV of 5% for cells with an antibody-secreting phenotype and 12% for cells with a memory B phenotype). We did not observe significant differences in the average and SD of the signal for each marker nor in the frequencies of the major immune compartments across repeated analyses.

### Statistical Analyses

Statistical significance was performed using GraphPad Prism or R. Statistical tests used are reported in the figure legends. Comparisons between DSA<sup>POS</sup>, DSA-negative recipients (DSA<sup>NEG</sup>), and DSA<sup>POS</sup>AMR-positive recipients (AMR<sup>POS</sup>) groups at the same time point were performed by unpaired *t* tests or ANOVA (nonparametric tests were also performed yielding similar results). Differences are considered significant at *P* < 0.05.

## RESULTS

### Recipients

All included subjects were unsensitized, first-time pediatric recipients of kidney transplants who received the same induction and similar immunosuppression therapy (Table 1).

Adherence to CNI maintenance immunosuppression, as determined by cyclosporine or tacrolimus IPV at 6 months posttransplant and onward, did not differ in DSA<sup>POS</sup> versus DSA<sup>NEG</sup> recipients or in DSA<sup>POS</sup> patients who developed (DSA<sup>POS</sup>AMR<sup>POS</sup>) or not (DSA<sup>POS</sup>AMR-negative recipients (AMR<sup>NEG</sup>)) AMR (Figure S1, SDC, <http://links.lww.com/TXD/A217>, see Adherence to CNI Therapy in the Materials and Methods section). The majority of patients received deceased donor renal transplants (Table 1). Ten recipients developed DSA posttransplant, and 11 remained DSA negative over the 5-year follow-up period. Baseline characteristics did not differ significantly between DSA<sup>POS</sup> and DSA<sup>NEG</sup> recipients (Table 1). Recipients who developed DSA had increased rates of acute cellular rejection, AMR, and graft loss during the 4-year follow-up period (Table 2).

### DSA Antibody Levels and C1q and C3d Binding

Baseline characteristics (Table S2, SDC, <http://links.lww.com/TXD/A217>) of MFI levels at the time of DSA detection ( $9.5 \pm 3.4$  mo posttransplant) were similar between recipients who did and did not develop AMR (Table S3, SDC, <http://links.lww.com/TXD/A217>;  $13\,686.6 \pm 9300.8$  vs  $11\,375.4 \pm 4234.5$ , respectively; *P* = 0.63). All DSA<sup>POS</sup> patients developed antibodies reactive against HLA class II antigens. Three recipients also had DSA against HLA class I, but those antibodies were developed either at the time of DSA detection (*n* = 1) or after the onset of class II DSA (*n* = 2; Table S3, SDC, <http://links.lww.com/TXD/A217>). DSA levels remained generally stable over time, except in 3 DSA<sup>POS</sup>AMR<sup>POS</sup> patients who showed an increase in their levels.

The majority of DSAs were targeted against HLA-DQ and bound C1q (Table 3). Three of the 5 DSA<sup>POS</sup>AMR<sup>POS</sup> recipients

**TABLE 1.**  
Baseline characteristics of donors and recipients

	Total (n = 21)	DSA <sup>POS</sup> (n = 10)	DSA <sup>NEG</sup> (n = 11)	<i>P</i>
<b>Donors</b>				
Age, y	15.0 ± 12.0	11.0 ± 5.8	18.5 ± 15.1	0.15
Male, n (%)	14 (67)	8 (80)	6 (54)	0.36
Living, n (%)	3 (33)	0 (0)	3 (27)	0.21
<b>Recipients</b>				
Age, y	10.9 ± 5.2	10.8 ± 6.4	10.9 ± 4.3	0.96
Male, n (%)	13 (62)	8 (80)	5 (46)	0.18
Race (%)				1.00
White	19 (90)	9 (90)	10 (91)	
Black	1 (5)	0 (0)	1 (9)	
Hispanic	1 (5)	1 (10)	0 (0)	
Primary renal disease, n (%)				0.22
Alport syndrome	1 (5)	1 (10)	0 (0)	
ANCA+ vasculitis	2 (10)	0 (0)	2 (18)	
ARPKD	2 (10)	2 (20)	0 (0)	
CAKUT	10 (48)	6 (60)	4 (36)	
FSGS	2 (10)	1 (10)	1 (9)	
Interstitial nephropathy	1 (5)	0 (0)	1 (9)	
Nephronophthisis	3 (14)	1 (10)	2 (18)	
Mo on dialysis	17.3 ± 11.1	17.2 ± 10.2	17.5 ± 12.4	0.96
Cold ischemia time, min	791.3 ± 309.9	816.8 ± 184.9	768.2 ± 400.0	0.72
HLA mismatch (A + B + DQ + DR)	4.5 ± 1.3	4.6 ± 1.3	4.4 ± 1.4	0.68

All donors were white. No patient had a peak panel-reactive antibody >20%. Continuous variables are represented as mean ± SD. Categorical variables are expressed as a percentage. ANCA, antineutrophil cytoplasmic antibodies; ARPKD, autosomal recessive polycystic kidney disease; CAKUT, congenital anomalies of the kidney and urinary tract; DSA, donor-specific antibody; DSA<sup>NEG</sup>, DSA-negative recipients; DSA<sup>POS</sup>, DSA-positive recipients; FSGS, focal segmental glomerulosclerosis; HLA, human leukocyte antigen; SD, standard deviation.

**TABLE 2.****Allograft outcomes of patients by DSA status**

	Total (n = 21)	DSA <sup>POS</sup> (n=10)	DSA <sup>NEG</sup> (n = 11)	P
eGFR posttransplant				
3 mo	102.7 ± 19.6	98.8 ± 24.9	106.2 ± 13.6	0.42
6 mo	101.9 ± 20.5	97.7 ± 24.9	105.8 ± 15.8	0.39
9 mo	98.2 ± 18.6	94.7 ± 22.7	101.3 ± 14.3	0.45
12 mo	98.2 ± 18.8	95.2 ± 23.2	100.8 ± 14.3	0.52
DGF, n (%)	2 (10)	1 (10)	1 (9)	1.00
ACR n (%)	3 (33)	3 (30)	0 (0)	0.09
ACR time posttransplant, mo	5 (24)	17.0 ± 1.0	N/A	0.01 <sup>a</sup>
AMR, n (%)		5 (50)	0 (0)	
AMR time posttransplant, mo		27.4 ± 8.0	N/A	
Graft loss, n (%)	3 (33)	3 (30)	0 (0)	0.09
Graft loss time posttransplant, mo		48.0 ± 25.1	N/A	

<sup>a</sup>P < 0.05 by unpaired *t* test for continuous variables or Fisher exact test for categorical variables.

eGFR was estimated via the Schwartz formula.<sup>46</sup> Categorical variables are expressed as a percentage. Continuous variables are represented as mean ± SD.

ACR, acute cellular rejection; AMR, antibody-mediated rejection; DGF, delayed graft function; DSA, donor-specific antibody; DSA<sup>NEG</sup>, DSA-negative recipients; DSA<sup>POS</sup>, DSA-positive recipients; eGFR, estimated glomerular filtration rate; N/A, non-applicable; SD, standard deviation.

had DSA that bound C3d upon initial DSA detection, while only 1 DSA<sup>POS</sup>AMR<sup>NEG</sup> recipient had C3d-binding DSA (Table 3).

### Frequencies of Major Immune Compartments

We analyzed the evolution of 9 major immune compartments in peripheral blood (Figure 2) using an unbiased algorithm (Phenograph<sup>49</sup>; see Materials and Methods section). The resultant high-dimensional clustered data were visualized in 2 dimensions with preserved single-cell resolution using viSNE (Figure 2A). Once all clusters were defined as belonging to a major immune compartment, the cellular frequencies were calculated for each patient at all time points.

Overall, cell frequencies of major immune compartments remained relatively stable throughout the 3 time points and were similar to the cell frequencies previously reported by our group in adult kidney transplant recipients during the first year after transplantation.<sup>46</sup> Major immune subsets were not significantly different between DSA<sup>POS</sup> and DSA<sup>NEG</sup> recipients except for monocytes, which were elevated in DSA<sup>POS</sup> recipients before DSA detection (Figure 2). While no single cluster reciprocally increased in the DSA<sup>NEG</sup> group, an increase in several lymphocyte populations in DSA<sup>NEG</sup> recipients collectively accounted for the elevated monocytes in DSA<sup>POS</sup> recipients before DSA development (Figure S2, SDC, <http://links.lww.com/TXD/A217>). B cells declined over time in both groups, but only DSA<sup>NEG</sup> subjects had a statistically significant decrease in total B cells from 2 months posttransplant to the time of DSA detection.

### DSA<sup>POS</sup> and DSA<sup>NEG</sup> Recipients Have Similar Frequencies of Circulating CD4<sup>+</sup> and CD8<sup>+</sup> T-Cell Subsets

Although we did not detect any significant differences between CD4<sup>+</sup> or CD8<sup>+</sup> T cells in DSA<sup>POS</sup> versus DSA<sup>NEG</sup> recipients (Figure 2), we performed a second level of unbiased clustering within those compartments using 20 additional markers to determine whether any subpopulations differed between the 2 recipient groups (Table S1, SDC, <http://links.lww.com/TXD/A217>; Figure 3A and B). The cells from all recipients were pooled together, and 8 CD4<sup>+</sup> (Figure 3A and B) and 7 CD8<sup>+</sup> (Figure 4A and B) T-cell subpopulations were defined based on relative expression of the clustering markers. The subclusters were then demultiplexed to extract the frequency of each subpopulation for each patient over time (Figures 3B and 4B). Similar to our findings for the major immune compartments, no significant differences in CD4<sup>+</sup> and CD8<sup>+</sup> T-cell subpopulations were detected.

Of note, CD4<sup>+</sup> T cells with a T-follicular helper-like (T<sub>FH</sub>) phenotype (see Figure 3, clusters 2, 11, and 19 for markers) were not increased in the peripheral circulation of DSA<sup>POS</sup> recipients despite their importance in antibody production.<sup>50,51</sup> The percentages of regulatory T cells (T<sub>REG</sub>) also did not significantly differ between DSA<sup>POS</sup> and DSA<sup>NEG</sup> recipients at the analyzed time points. When we stratified DSA<sup>POS</sup> recipients according to the future development of AMR, we could not

**TABLE 3.****DSA specificities for DSA<sup>POS</sup> recipients**

	Total (n = 10)	AMR <sup>POS</sup> (n = 5)	AMR <sup>NEG</sup> (n = 5)	P
HLA specificity		DQ5 DQ6 DQA1 0505 <sup>a</sup> DQ8 <sup>a</sup> DQ9 A2 B58 B37 DR10 <sup>a</sup>	DQA1 0501 DQ7 DQ7 DQ5 DQ2	
C1q binding, n (%)	9 (90)	5 (100)	4 (80)	1.00
C3d binding, n (%)	4 (40)	3 (60)	1 (20)	0.52

<sup>a</sup>Recipients who lost their grafts.

Recipients not listed in any particular order. Variables are expressed as a percentage.

AMR, antibody-mediated rejection; AMR<sup>NEG</sup>, AMR negative patients; AMR<sup>POS</sup>, AMR positive patients; DSA, donor-specific antibody; DSA<sup>POS</sup>, DSA-positive recipients; HLA, human leukocyte antigen.

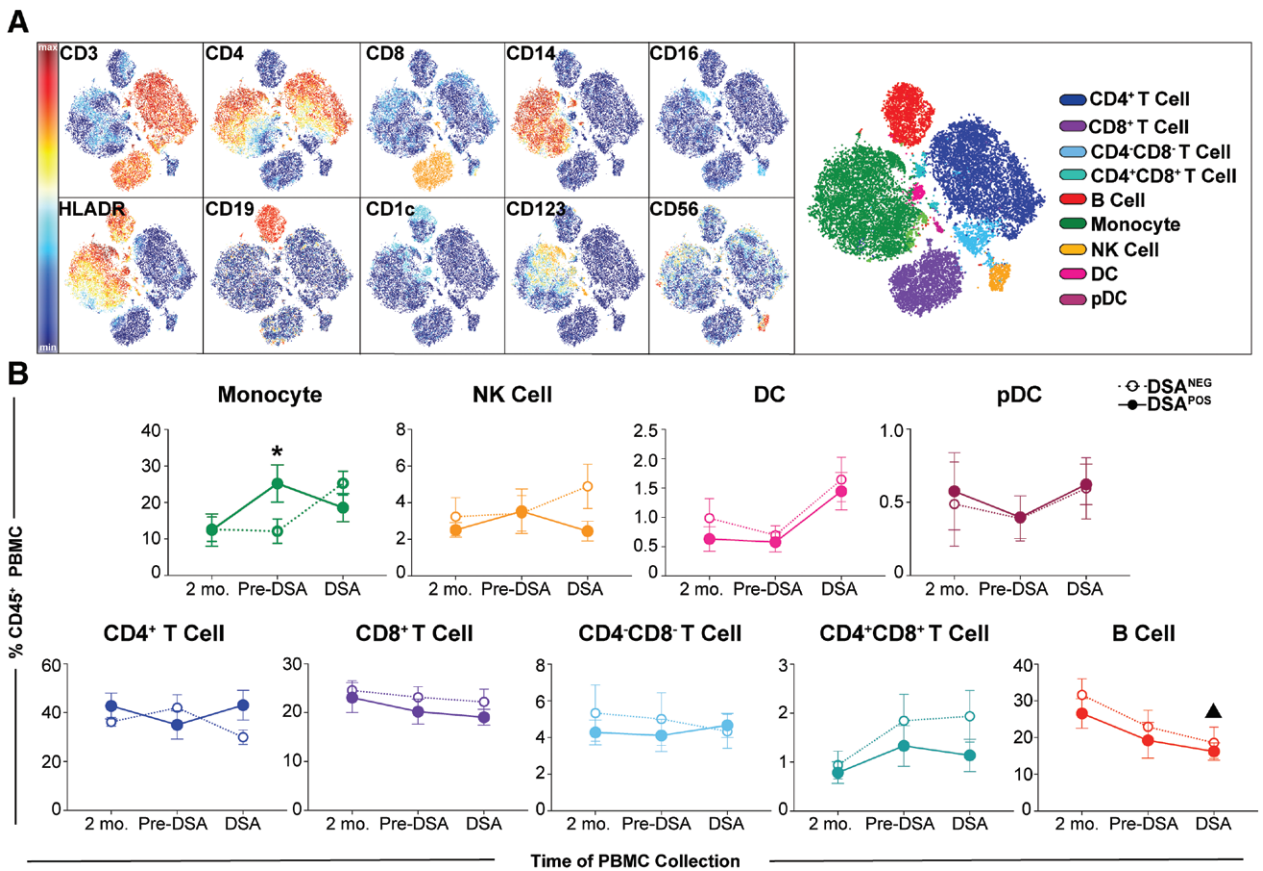


**FIGURE 2.** Frequencies of major immune compartments. A, Representative viSNE plots of peripheral blood mononuclear cells (PBMC) colored by their relative expression of cell markers used to define major immune clusters (populations defined on the right). B, Percentages of major immune compartments based on the summation of Phenograph clusters (see Materials and Methods,  $n = 21$  subjects). Error bars represent SEM. Comparisons between DSA<sup>POS</sup> and DSA<sup>NEG</sup> (\* $P < 0.05$ , \*\* $P < 0.01$  by unpaired  $t$  test) and with baseline (▲ $P < 0.05$  by paired  $t$  test). DC, Dendritic Cells; DSA, donor-specific antibody; DSA<sup>NEG</sup>, DSA-negative recipients; DSA<sup>POS</sup>, DSA-positive recipients; NK, Natural Killer; pDC, Plasmacytoid Dendritic Cells; SEM, standard error of the mean.

detect any significant differences in any of the CD4<sup>+</sup> or CD8<sup>+</sup> T-cell compartments (not shown).

### B Cells With Antibody-Secreting and Memory Phenotypes Are Increased in DSA<sup>POS</sup> Recipients Before AMR Development

Within the B-cell compartment, we identified 10 distinct B-cell subpopulations, including B cells with a naive (IgD<sup>+</sup>CD27<sup>-</sup>),<sup>52</sup> regulatory (CD25<sup>hi</sup>),<sup>53,54</sup> antibody-secreting (IgD<sup>-</sup>CD27<sup>+</sup>CD38<sup>+</sup>),<sup>55</sup> and memory (IgD<sup>-</sup>CD27<sup>+</sup>CD38<sup>-</sup>)<sup>52</sup> phenotype. We did not detect statistically significant differences at any time point in B-cell subpopulations between DSA<sup>POS</sup> and DSA<sup>NEG</sup> recipients (Figure 5B).

However, we noticed a trend toward increased B cells with antibody-secreting or memory phenotypes at the time of DSA in DSA<sup>POS</sup> recipients compared with DSA<sup>NEG</sup> individuals. We then hypothesized that stratification of DSA<sup>POS</sup> recipients according to the development of AMR within the first 5 years posttransplant would elucidate cells potentially responsible for this immunological process. B cells with antibody-secreting or memory phenotypes were significantly increased at the time of DSA detection only in DSA<sup>POS</sup> recipients that later developed AMR (Figure 6). Of note, these cells were present in the peripheral blood  $\approx 18$  months before the onset of AMR diagnosis by biopsy (Table 2). None of the major immune compartments differed significantly at any time points between

DSA<sup>POS</sup> patients who did or did not develop AMR. DSA levels at 2 and 3 years after transplant in DSA<sup>POS</sup> patients who developed AMR did not significantly differ compared with those of DSA<sup>POS</sup> patients who did not develop AMR (DSA at 2 y:  $12\,170 \pm 7722$  vs  $8540 \pm 7799$ ,  $P = 0.48$ ; at 3 y:  $11\,970 \pm 3997$  vs  $11\,600 \pm 7214$  MFI;  $P = 0.92$ , respectively). The 3 patients who lost their grafts developed AMR and had high levels of B cells with antibody-secreting and memory phenotypes.

### DISCUSSION

Identifying cellular immune mediators responsible for AMR in kidney transplant recipients has proven difficult due to the limited number of markers that can be probed using flow cytometry. We utilized unbiased CyTOF analyses to comprehensively characterize the immune phenotype in pediatric kidney transplant recipients using serial samples collected before and at the time of DSA development. While CyTOF has been used with great success in the oncologic sciences, its implementation in human solid organ transplantation has been limited to a few studies.<sup>46,56</sup> Herein, we discovered that, while percentages of circulating B cells with an antibody-secreting or memory phenotype did not significantly differ between DSA<sup>POS</sup> and DSA<sup>NEG</sup> recipients before DSA detection, they were enriched at the time of DSA detection only in recipients who developed AMR >1 year later.

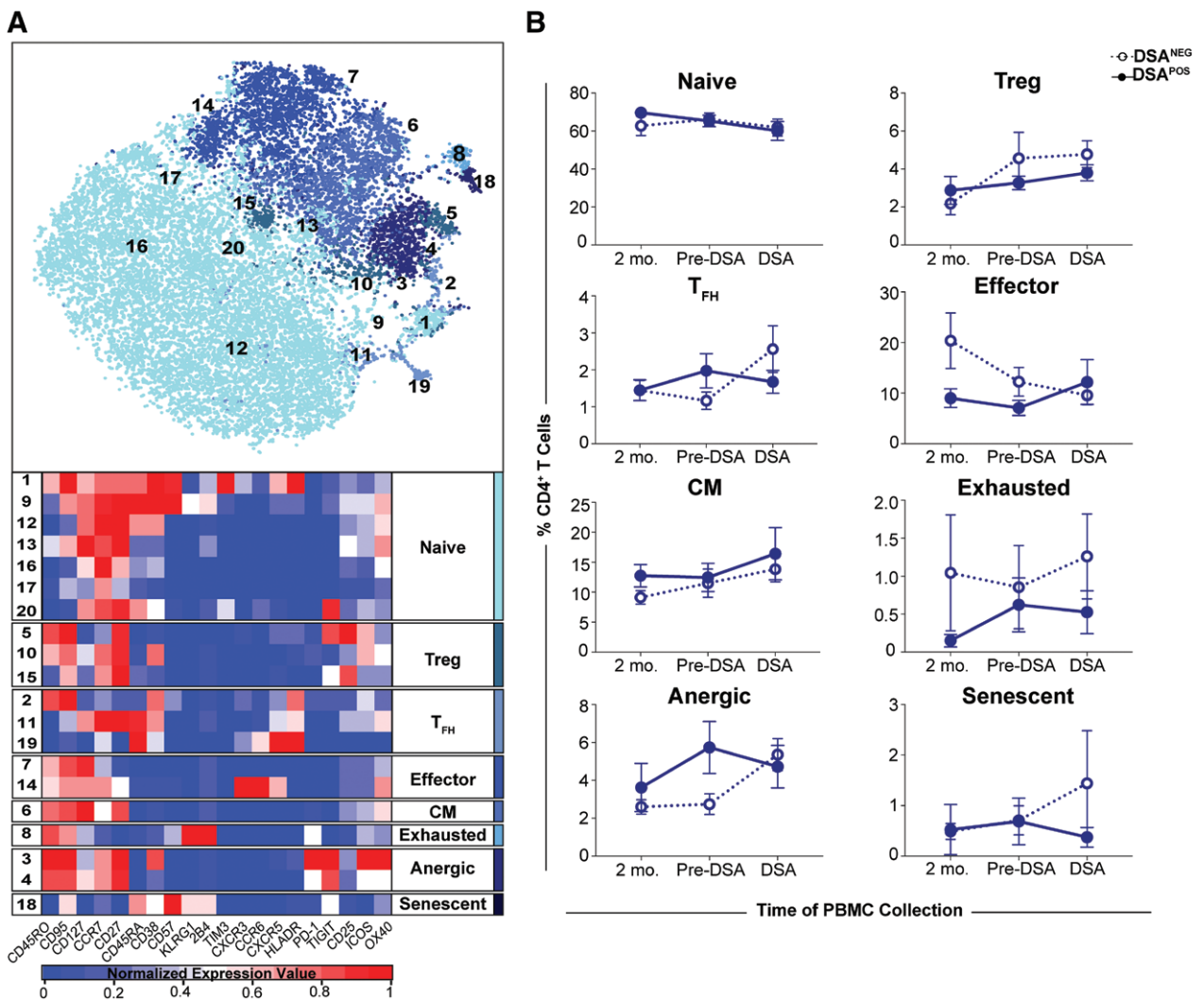


**FIGURE 3.** CD4<sup>+</sup> T-cell subpopulations did not differ between DSA<sup>POS</sup> and DSA<sup>NEG</sup> recipients. A, viSNE analysis of CD3<sup>+</sup>CD4<sup>+</sup> T-cell subpopulations (top) labeled by Phenograph clustering analysis and corresponding heatmap assignment (bottom) for all subjects and time points combined (see Materials and Methods). B, Analysis of the percentages of 8 CD4<sup>+</sup> subpopulations (see Materials and Methods, n = 21 subjects). Error bars represent SEM. Comparisons at all time points were not significantly different (unpaired *t* test). CM, Central Memory; DSA, donor-specific antibody; DSA<sup>NEG</sup>, DSA-negative recipients; DSA<sup>POS</sup>, DSA-positive recipients; PBMC, peripheral blood mononuclear cells; SEM, standard error of the mean; T<sub>FH</sub>, T-follicular helper-like; T<sub>REG</sub>, regulatory T cells.

It is well established that DSA positivity portends inferior allograft outcomes due to the increased risk of AMR.<sup>8,57,58</sup> However, the factors leading to dnDSA development and progression to AMR are unclear. Half of the DSA<sup>POS</sup> recipients in our cohort developed AMR despite similar baseline characteristics, immunosuppression regimens, and donor/recipient HLA matches (Table 1). Nonadherence has been implied as a major risk factor for the development of DSA, especially in pediatric recipients.<sup>43,44</sup> IPV in cyclosporine and tacrolimus levels was within target ranges and similar across all recipients (Figure S1, SDC, <http://links.lww.com/TXD/A217>), suggesting that nonadherence was not a major determinant for dnDSA development in our cohort.<sup>42-44</sup>

DSA levels at the time of DSA detection were similar as well, making this information of little value to risk-stratify DSA recipients who will develop AMR (Table S3, SDC, <http://links.lww.com/TXD/A217>). Others have reported that the ability to fix and activate the complement cascade, as determined by C1q and C3d binding, identifies pathogenic

DSA and correlates with shorter allograft survival.<sup>21,23-27,59,60</sup> However, 9 out of the 10 recipients in our cohort had DSA that bound C1q (Table 3). More DSA<sup>POS</sup>AMR<sup>POS</sup> recipients had C3d-binding DSA, but this trend did not reach statistical significance (*P* = 0.52). Therefore, in this pediatric population, C1q and C3d staining did not prove to be useful predictors of AMR development.

B cells with memory or antibody-secreting phenotype were the only cell subsets that we identified as differentially increased in DSA<sup>POS</sup> recipients that later developed AMR. These cells were identified based on their absence of IgD and expression of CD27—signifying mature B cells<sup>61</sup>—and differential expression of CD38. CD38 is a highly conserved type II glycoprotein that possesses pleiotropic effects on B-cell function and maturation.<sup>62-64</sup> Whereas CD38 induces apoptosis in early B cells, it promotes survival in germinal center B cells.<sup>65</sup> Antibody-secreting cells, including plasma cells and immature plasmablasts,<sup>66</sup> express high levels of CD38, whereas memory B cells, a long-lasting B-cell subset capable of differentiating into antibody-secreting B cells and producing high-affinity antibodies

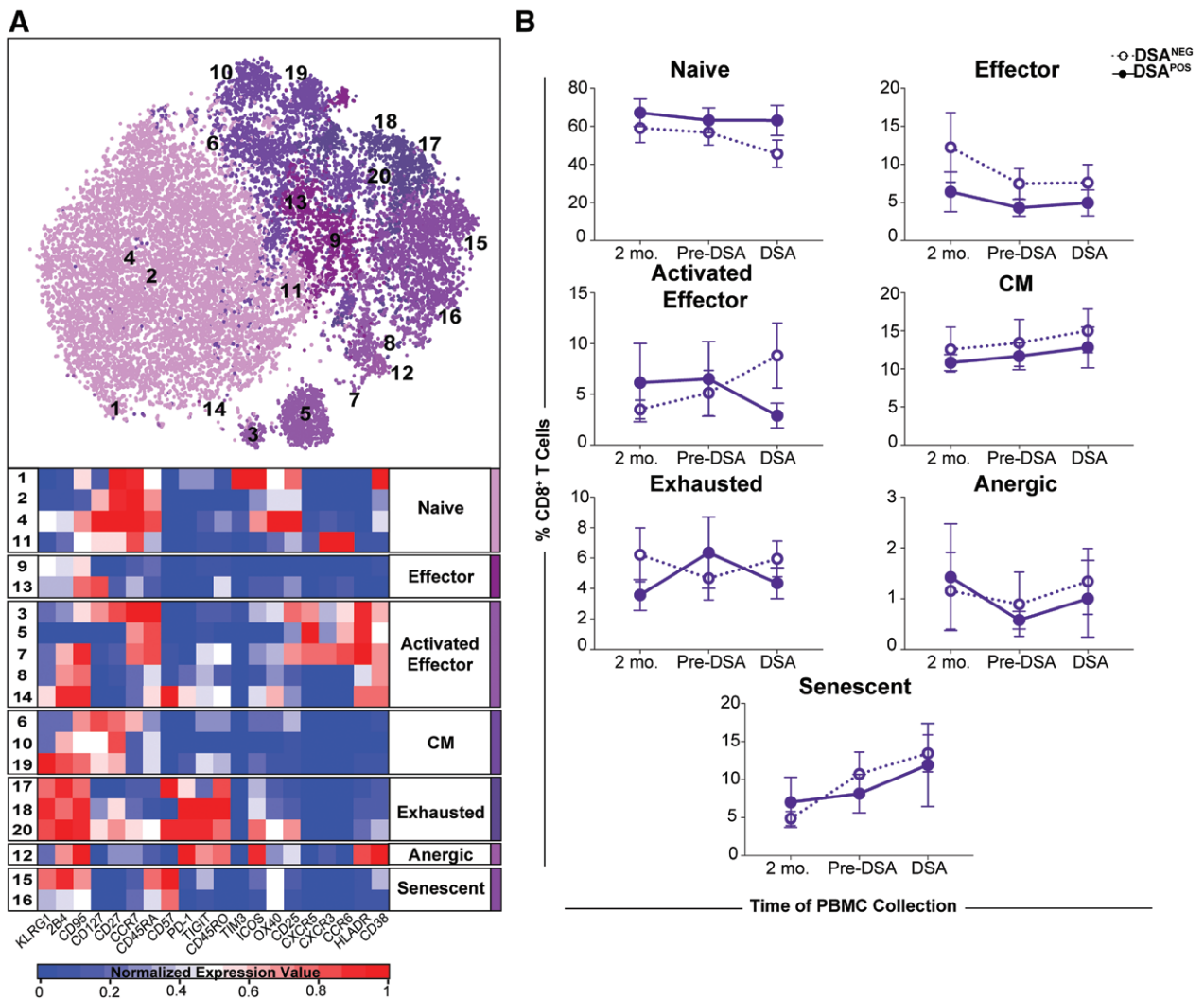


**FIGURE 4.** CD8<sup>+</sup> T-cell subpopulations did not differ between DSA<sup>POS</sup> and DSA<sup>NEG</sup> recipients. A, viSNE analysis of CD3<sup>+</sup>CD8<sup>+</sup> T cell subpopulations (top) labeled by Phenograph clustering analysis and corresponding heatmap assignment (bottom) for all subjects and time points combined (see Materials and Methods). B, Analysis of the percentages of 7 CD8<sup>+</sup> subpopulations (see Materials and Methods, *n* = 21 subjects). Error bars represent SEM. Comparisons at all time points were not significantly different (unpaired *t* test). CM, Central Memory; DSA, donor-specific antibody; DSA<sup>NEG</sup>, DSA-negative recipients; DSA<sup>POS</sup>, DSA-positive recipients; PBMC, peripheral blood mononuclear cells; SEM, standard error of the mean.

upon antigen re-encounter,<sup>33-35</sup> lack CD38 expression.<sup>67,68</sup> Our data confirm and expand to a pediatric population previous evidence by Luque et al<sup>52</sup> showing increased donor-reactive memory B cells in the circulation of adult DSA<sup>POS</sup> recipients with ongoing AMR. Intriguingly, these authors identified donor-reactive memory B cells by Elispot, while they failed to identify a difference in any of the B cell subsets measured by flow cytometry.<sup>52</sup> The increased sensitivity of the CyTOF technique when compared with flow cytometry provides the opportunity to identify and quantify low-frequency lymphocyte populations in peripheral blood. Indeed, we were able to probe for differences in 9 major immune compartments and 25 lymphocyte subpopulations using CyTOF.

Our comprehensive immune phenotypic characterization by CyTOF also allowed us to test for any relationship between circulating T-cell subsets and DSA development. Unexpectedly, we did not detect differences in any of the CD4<sup>+</sup> or CD8<sup>+</sup> T-cell subsets between DSA<sup>POS</sup> and DSA<sup>NEG</sup> recipients at any time point, including circulating T<sub>FH</sub>—a specialized T-cell subset integral to efficient antibody

production that assists B-cell differentiation into plasma cells—and T<sub>REG</sub>. Different groups have attempted to find a relationship between circulating T<sub>FH</sub> or T<sub>REG</sub> and graft outcomes, but results, invariably generated using flow cytometry, have been inconsistent so far.<sup>52,69-72</sup> Our comprehensive, unbiased approach on serially collected samples does not support such a relationship, at least in pediatric patients.

Our study has some limitations. The sample size was relatively small, and we did not validate our results in an independent cohort. However, we resampled and reanalyzed the B-cell clusters 5 times to ensure that our findings were statistically robust. CyTOF allowed us to conduct comprehensive immune phenotyping with increased sensitivity for low-expressed markers. Although perfectly suited to extract the most information from a reduced number of samples, it cannot overcome the limitations associated with a small number of patients. We also have not determined that the B cells with a memory or antibody-secreting phenotype are specific to the HLA antigens that the DSAs were against. Lack of functional data on B cells with a memory or antibody-secreting



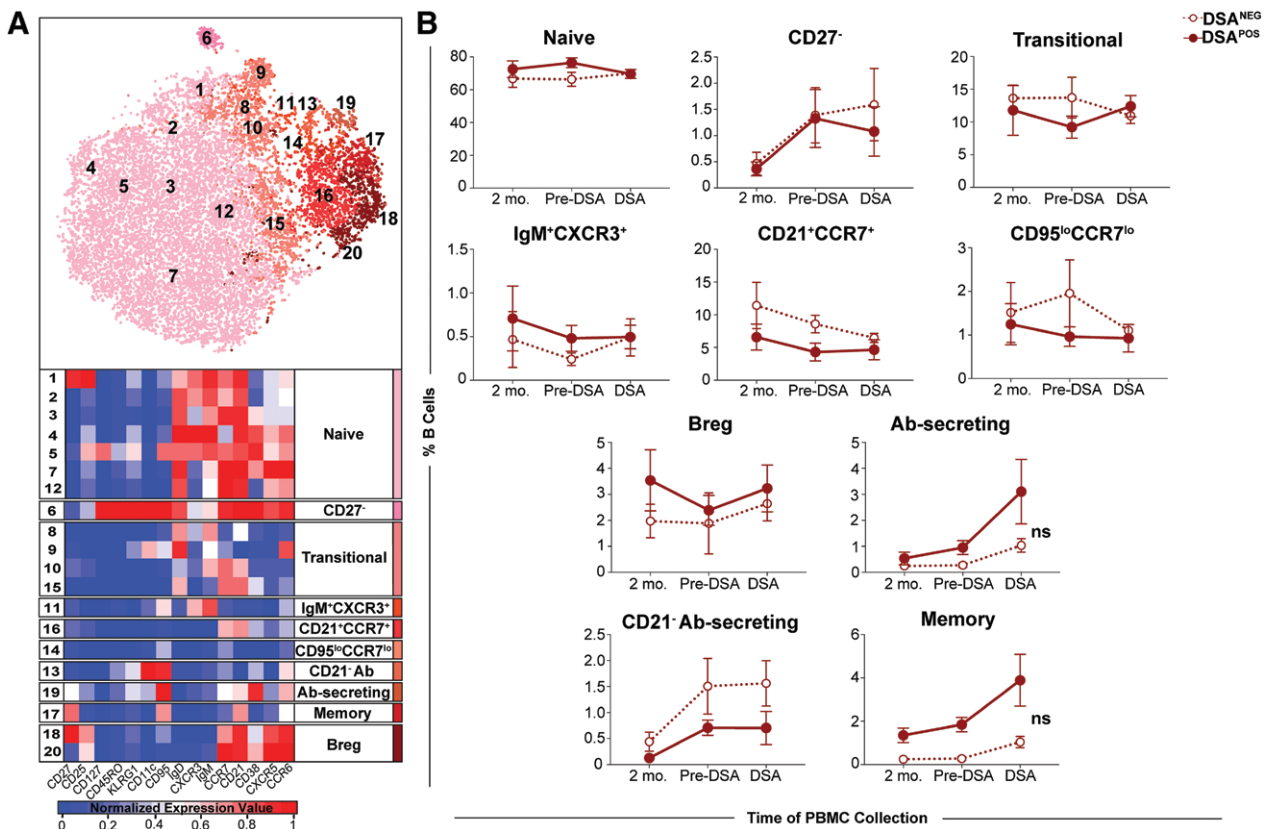


**FIGURE 5.** B-cell subpopulations were similar in DSA<sup>POS</sup> and DSA<sup>NEG</sup> recipients. A, viSNE analysis of CD19<sup>+</sup> B-cell subpopulations (top) labeled by Phenograph cluster and corresponding heatmap assignment (bottom) for all subjects and time points combined (see Materials and Methods). B, Analysis of the percentages of 10 B-cell subpopulations (see Materials and Methods, n = 21 subjects). Error bars represent SEM. Comparisons at all time points were not significantly different (unpaired *t* test). Ab, antibody; Breg, regulatory B cells; DSA, donor-specific antibody; DSA<sup>NEG</sup>, DSA-negative recipients; DSA<sup>POS</sup>, DSA-positive recipients; PBMC, peripheral blood mononuclear cells; SEM, standard error of the mean.

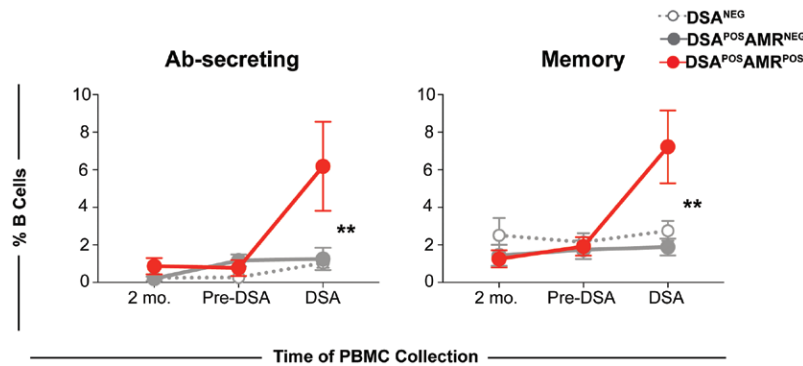


**FIGURE 6.** B cells with antibody-secreting and memory phenotype were increased at the time of DSA detection only in DSA<sup>POS</sup> patients who later developed AMR. Analysis of the percentages of antibody-secreting (left) and memory B cell (right) subpopulations stratified by DSA and AMR status (see Materials and Methods, n = 21 subjects). Error bars represent SEM. \**P* < 0.05, \*\**P* < 0.01 by ANOVA. Ab, antibody; AMR, antibody-mediated rejection; AMR<sup>NEG</sup>, AMR negative recipients; AMR<sup>POS</sup>, AMR positive; DSA, donor-specific antibody; DSA<sup>POS</sup>, DSA-positive recipients; PBMC, peripheral blood mononuclear cells; SEM, standard error of the mean.

phenotype represents another limitation, although the cell surface markers used to classify these cells are well established in the literature.<sup>67,68</sup> Our phenotypic data complement functional studies by others showing that memory B cells can be detected in the circulation before DSA development.<sup>52</sup> Future studies will be required to define antigen specificity of B cells with memory or antibody-secreting phenotype.

Overall, the present study demonstrates that circulating B cells with an antibody-secreting and memory phenotype increase in DSA<sup>POS</sup> recipients before the development of AMR. We also show

that these cells are detectable in the peripheral circulation at the time of DSA onset, more than a year before biopsy-proven rejection, highlighting a possible role for aggressive B-cell-targeted immunosuppression in these at-risk recipients. These pilot results warrant further validation in larger cohort studies.

**REFERENCES**

1. Kidney Disease: Improving Global Outcomes (KDIGO) Transplant Work Group. KDIGO clinical practice guideline for the care of kidney transplant recipients. *Am J Transplant.* 2009;9(Suppl 3):S1–S155.

2. Kasiske BL, Zeier MG, Chapman JR, et al. Kidney Disease: Improving Global Outcomes. KDIGO clinical practice guideline for the care of kidney transplant recipients: a summary. *Kidney Int.* 2010;77:299–311.
3. Lamb KE, Lodhi S, Meier-Kriesche HU. Long-term renal allograft survival in the United States: a critical reappraisal. *Am J Transplant.* 2011;11:450–462.
4. Lodhi SA, Lamb KE, Meier-Kriesche HU. Solid organ allograft survival improvement in the United States: the long-term does not mirror the dramatic short-term success. *Am J Transplant.* 2011;11:1226–1235.
5. Meier-Kriesche HU, Schold JD, Srinivas TR, et al. Lack of improvement in renal allograft survival despite a marked decrease in acute rejection rates over the most recent era. *Am J Transplant.* 2004;4:378–383.
6. Van Arendonk KJ, Boyarsky BJ, Orandi BJ, et al. National trends over 25 years in pediatric kidney transplant outcomes. *Pediatrics.* 2014;133:594–601.
7. Zhang R. Donor-specific antibodies in kidney transplant recipients. *Clin J Am Soc Nephrol.* 2018;13:182–192.
8. Wiebe C, Gibson IW, Blydt-Hansen TD, et al. Evolution and clinical pathologic correlations of de novo donor-specific HLA antibody post kidney transplant. *Am J Transplant.* 2012;12:1157–1167.
9. Hart A, Smith JM, Skeans MA, et al. Kidney. *Am J Transplant.* 2016;16(Suppl 2):11–46.
10. Hart A, Smith JM, Skeans MA, et al. OPTN/SRTR 2016 Annual Data Report: kidney. *Am J Transplant.* 2018;18(Suppl 1):18–113.
11. Chehade H, Pascual M. The challenge of acute antibody-mediated rejection in kidney transplantation. *Transplantation.* 2016;100:264–265.
12. Montgomery RA, Loupy A, Segev DL. Antibody-mediated rejection: new approaches in prevention and management. *Am J Transplant.* 2018;18(Suppl 3):3–17.
13. Gaston RS, Cecka JM, Kasiske BL, et al. Evidence for antibody-mediated injury as a major determinant of late kidney allograft failure. *Transplantation.* 2010;90:68–74.
14. Nankivell BJ, Kuypers DR. Diagnosis and prevention of chronic kidney allograft loss. *Lancet.* 2011;378:1428–1437.
15. Sautenet B, Blanco G, Büchler M, et al. One-year results of the effects of rituximab on acute antibody-mediated rejection in renal transplantation: RITUX ERAH, a multicenter double-blind randomized placebo-controlled trial. *Transplantation.* 2016;100:391–399.
16. Valenzuela NM, Reed EF. Antibodies in transplantation: the effects of HLA and Non-HLA antibody binding and mechanisms of injury. In: Zachary AA, Lefell MS, editors. *Transplantation Immunology: Methods and Protocols.* Totowa, NJ: Humana Press; 2013:41–70.
17. Kosmoliaptsis V, Sharples LD, Chaudhry AN, et al. Predicting HLA class II alloantigen immunogenicity from the number and physicochemical properties of amino acid polymorphisms. *Transplantation.* 2011;91:183–190.
18. Loupy A, Vernerey D, Tinel C, et al. Subclinical rejection phenotypes at 1 year post-transplant and outcome of kidney allografts. *J Am Soc Nephrol.* 2015;26:1721–1731.
19. Kumbala D, Zhang R. Essential concept of transplant immunology for clinical practice. *World J Transplant.* 2013;3:113–118.
20. Thomas KA, Valenzuela NM, Reed EF. The perfect storm: HLA antibodies, complement, fcγrs, and endothelium in transplant rejection. *Trends Mol Med.* 2015;21:319–329.
21. Comoli P, Cioni M, Tagliamacco A, et al. Acquisition of C3d-binding activity by de novo donor-specific HLA antibodies correlates with graft loss in nonsensitized pediatric kidney recipients. *Am J Transplant.* 2016;16:2106–2116.
22. Chen G, Sequeira F, Tyan DB. Novel C1Q assay reveals a clinically relevant subset of human leukocyte antigen antibodies independent of immunoglobulin G strength on single antigen beads. *Hum Immunol.* 2011;72:849–858.
23. Yabu JM, Higgins JP, Chen G, et al. C1q-fixing human leukocyte antigen antibodies are specific for predicting transplant glomerulopathy and late graft failure after kidney transplantation. *Transplantation.* 2011;91:342–347.
24. Freitas MC, Rebollato LM, Ozawa M, et al. The role of immunoglobulin-G subclasses and C1Q in de novo HLA-DQ donor-specific antibody kidney transplantation outcomes. *Transplantation.* 2013;95:1113–1119.
25. Sutherland SM, Chen G, Sequeira FA, et al. Complement-fixing donor-specific antibodies identified by a novel C1Q assay are associated with allograft loss. *Pediatr Transplant.* 2012;16:12–17.
26. Sicard A, Ducreux S, Rabeyrin M, et al. Detection of C3d-binding donor-specific anti-HLA antibodies at diagnosis of humoral rejection predicts renal graft loss. *J Am Soc Nephrol.* 2015;26:457–467.
27. Loupy A, Lefaucheur C, Vernerey D, et al. Complement-binding anti-HLA antibodies and kidney-allograft survival. *N Engl J Med.* 2013;369:1215–1226.
28. Lee H, Han E, Choi AR, et al. Clinical impact of complement (C1q, C3d) binding de novo donor-specific HLA antibody in kidney transplant recipients. *PLoS One.* 2018;13:e0207434.
29. Okabe Y, Noguchi H, Miyamoto K, et al. Preformed C1q-binding donor-specific anti-HLA antibodies and graft function after kidney transplantation. *Transplant Proc.* 2018;50:3460–3466.
30. Moreno Gonzales MA, Mitea DG, Smith BH, et al. Comparison between total IgG, C1q, and C3d single antigen bead assays in detecting class I complement-binding anti-HLA antibodies. *Transplant Proc.* 2017;49:2031–2035.
31. Bamouid J, Roodenburg A, Staack O, et al. Clinical outcome of patients with de novo C1q-binding donor-specific HLA antibodies after renal transplantation. *Transplantation.* 2017;101:2165–2174.
32. Guidicelli G, Guerville F, Lepreux S, et al. Non-complement-binding de novo donor-specific anti-HLA antibodies and kidney allograft survival. *J Am Soc Nephrol.* 2016;27:615–625.
33. Buisman AM, de Rond CG, Oztürk K, et al. Long-term presence of memory B-cells specific for different vaccine components. *Vaccine.* 2009;28:179–186.
34. Crotty S, Aubert RD, Glidewell J, et al. Tracking human antigen-specific memory B cells: a sensitive and generalized ELISPOT system. *J Immunol Methods.* 2004;286:111–122.
35. Tarlinton D, Good-Jacobson K. Diversity among memory B cells: origin, consequences, and utility. *Science.* 2013;341:1205–1211.
36. McHeyzer-Williams MG, Ahmed R. B cell memory and the long-lived plasma cell. *Curr Opin Immunol.* 1999;11:172–179.
37. Chong AS, Sciammas R. Memory B cells in transplantation. *Transplantation.* 2015;99:21–28.
38. Lúcia M, Luque S, Crespo E, et al. Preformed circulating HLA-specific memory B cells predict high risk of humoral rejection in kidney transplantation. *Kidney Int.* 2015;88:874–887.
39. Haas M, Sis B, Racusen LC, et al; Banff Meeting Report Writing Committee. Banff 2013 meeting report: inclusion of c4d-negative antibody-mediated rejection and antibody-associated arterial lesions. *Am J Transplant.* 2014;14:272–283.
40. Tagliamacco A, Cioni M, Comoli P, et al. DQ molecules are the principal stimulators of de novo donor-specific antibodies in nonsensitized pediatric recipients receiving a first kidney transplant. *Transpl Int.* 2014;27:667–673.
41. Visentini J, Vigata M, Daburon S, et al. Deciphering complement interference in anti-human leukocyte antigen antibody detection with flow beads assays. *Transplantation.* 2014;98:625–631.
42. Shuker N, van Gelder T, Hesselink DA. Intra-patient variability in tacrolimus exposure: causes, consequences for clinical management. *Transplant Rev (Orlando).* 2015;29:78–84.
43. van Gelder T. Within-patient variability in immunosuppressive drug exposure as a predictor for poor outcome after transplantation. *Kidney Int.* 2014;85:1267–1268.
44. Prytula AA, Bouts AH, Mathot RA, et al. Intra-patient variability in tacrolimus trough concentrations and renal function decline in pediatric renal transplant recipients. *Pediatr Transplant.* 2012;16:613–618.
45. Lavin Y, Kobayashi S, Leader A, et al. Innate immune landscape in early lung adenocarcinoma by paired single-cell analyses. *Cell.* 2017;169:750.e17–765.e17.
46. Fribourg F, Fischman C, Anderson L, et al. T-cell exhaustion in kidney transplant patients. In: Paper presented at: American Transplant Congress; Seattle, Washington; June 5, 2018.
47. DiGiuseppe JA, Cardinali JL, Rezuze WN, et al. Phenograph and visne facilitate the identification of abnormal T-cell populations in routine clinical flow cytometric data. *Cytometry B Clin Cytom.* 2018;94:588–601.
48. Schwartz GJ, Haycock GB, Edelmann CM Jr, et al. A simple estimate of glomerular filtration rate in children derived from body length and plasma creatinine. *Pediatrics.* 1976;58:259–263.
49. Levine JH, Simonds EF, Bendall SC, et al. Data-driven phenotypic dissection of AML reveals progenitor-like cells that correlate with prognosis. *Cell.* 2015;162:184–197.
50. Campbell DJ, Kim CH, Butcher EC. Separable effector T cell populations specialized for B cell help or tissue inflammation. *Nat Immunol.* 2001;2:876–881.

51. Qi H. T follicular helper cells in space-time. *Nat Rev Immunol.* 2016;16:612–625.
52. Luque S, Lúcia M, Melilli E, et al. Value of monitoring circulating donor-reactive memory B cells to characterize antibody-mediated rejection after kidney transplantation. *Am J Transplant.* 2019;19:368–380.
53. Rosser EC, Mauri C. Regulatory B cells: origin, phenotype, and function. *Immunity.* 2015;42:607–612.
54. van de Veen W, Stanic B, Yaman G, et al. IgG4 production is confined to human IL-10-producing regulatory B cells that suppress antigen-specific immune responses. *J Allergy Clin Immunol.* 2013;131:1204–1212.
55. Matsumoto M, Baba A, Yokota T, et al. Interleukin-10-producing plasmablasts exert regulatory function in autoimmune inflammation. *Immunity.* 2014;41:1040–1051.
56. Yabu JM, Siebert JC, Maecker HT. Immune profiles to predict response to desensitization therapy in highly HLA-sensitized kidney transplant candidates. *PLoS One.* 2016;11(4):e0153355.
57. Worthington JE, Martin S, Al-Husseini DM, et al. Posttransplantation production of donor HLA-specific antibodies as a predictor of renal transplant outcome. *Transplantation.* 2003;75:1034–1040.
58. Lefaucheur C, Loupy A, Hill GS, et al. Preexisting donor-specific HLA antibodies predict outcome in kidney transplantation. *J Am Soc Nephrol.* 2010;21:1398–1406.
59. Bartel G, Wahrmann M, Schwaiger E, et al. Solid phase detection of C4d-fixing HLA antibodies to predict rejection in high immunological risk kidney transplant recipients. *Transpl Int.* 2013;26:121–130.
60. Lawrence C, Willicombe M, Brookes PA, et al. Preformed complement-activating low-level donor-specific antibody predicts early antibody-mediated rejection in renal allografts. *Transplantation.* 2013;95:341–346.
61. Jacquot S. CD27/CD70 interactions regulate T dependent B cell differentiation. *Immunol Res.* 2000;21:23–30.
62. Funaro A, Spagnoli GC, Ausiello CM, et al. Involvement of the multiligand CD38 molecule in a unique pathway of cell activation and proliferation. *J Immunol.* 1990;145:2390–2396.
63. Zupo S, Rugari E, Dono M, et al. CD38 signaling by agonistic monoclonal antibody prevents apoptosis of human germinal center B cells. *Eur J Immunol.* 1994;24:1218–1222.
64. Deaglio S, Vaisitti T, Bergui L, et al. CD38 and CD100 lead a network of surface receptors relaying positive signals for B-CLL growth and survival. *Blood.* 2005;105:3042–3050.
65. Deaglio S, Capobianco A, Bergui L, et al. CD38 is a signaling molecule in B-cell chronic lymphocytic leukemia cells. *Blood.* 2003;102:2146–2155.
66. Nutt SL, Hodgkin PD, Tarlinton DM, et al. The generation of antibody-secreting plasma cells. *Nat Rev Immunol.* 2015;15:160–171.
67. Jelinek DF, Splawski JB, Lipsky PE. Human peripheral blood B lymphocyte subpopulations: functional and phenotypic analysis of surface IgD positive and negative subsets. *J Immunol.* 1986;136:83–92.
68. Liu YJ, Barthélémy C, de Bouteiller O, et al. Memory B cells from human tonsils colonize mucosal epithelium and directly present antigen to T cells by rapid up-regulation of B7-1 and B7-2. *Immunity.* 1995;2:239–248.
69. Cano-Romero FL, Laguna Goya R, Utrero-Rico A, et al. Longitudinal profile of circulating T follicular helper lymphocytes parallels anti-HLA sensitization in renal transplant recipients. *Am J Transplant.* 2019;19:89–97.
70. de Graav GN, Dieterich M, Hesselink DA, et al. Follicular T helper cells and humoral reactivity in kidney transplant patients. *Clin Exp Immunol.* 2015;180:329–340.
71. Chenouard A, Chesneau M, Bui Nguyen L, et al. Renal operational tolerance is associated with a defect of blood tfh cells that exhibit impaired B cell help. *Am J Transplant.* 2017;17:1490–1501.
72. Alberu J, Vargas-Rojas MI, Morales-Buenrostro LE, et al. De novo donor-specific HLA antibody development and peripheral CD4(+) CD25(high) cells in kidney transplant recipients: a place for interaction? *J Transplant.* 2012;2012:302539.